Effect of acetic acid, methanol and potassium hydroxide on the catalytic steam reforming of glycerol: Thermodynamic and experimental study.

J. Remón, V. Mercado, L. García *, J. Arauzo

Thermochemical Processes Group (GPT), Aragon Institute for Engineering Research (I3A), Universidad de Zaragoza, Mariano Esquillor S/N, 50018 Zaragoza, Spain
* Corresponding author: e-mail: luciag@unizar.es Tel.: +34 976 762194

ABSTRACT

The present work analyses the effect on the reforming process of biodiesel crude glycerol of three impurities commonly found in this product. The influence of the presence of CH_3OH (0-5 wt.%) and/or CH_3COOH (0-3 wt.%) and/or KOH (0-2.8 wt.%) during the catalytic steam reforming of a 30 wt.% glycerol aqueous solution has been evaluated theoretically, studying the equilibrium composition of the gas, and experimentally in a fluidised bed reactor at 550 ºC. The presence of the aforementioned impurities has a weak impact on the thermodynamic gas composition. However, they significantly influence the product distribution (in carbon basis) obtained experimentally. The carbon of the feed converted into gas, solid and liquid products varied as follows: 75-100 %, 0-25% and 0-2.5%. CH_3OH alone does not alter the results obtained with pure glycerol. In contrast, CH_3COOH and KOH decrease the initial production of gases. This decrease is very high for KOH due to the formation of char. However, its progressive accumulation inside the reactor exerts a positive catalytic effect on the gasification of this char, augmenting the gas production over time. The composition of the gas was little affected by the presence of the impurities. The gas phase was made up of a mixture of H_2 (66-70 vol.%), CO_2 (24-29 vol.%), CO (3-6 vol.%) and CH_4 (0.5-2.5 vol.%). The liquid phase consisted of a mixture of alcohols, ketones, cyclic compounds, aldehydes and phenols.

Keywords: glycerol, acetic acid, methanol, potassium hydroxide, steam reforming.

1. Introduction

As a result of environmental concerns and stricter regulations for fuels, worldwide biodiesel production is increasing dramatically. In the biodiesel production process, glycerol is obtained as a by-product (10 kg of biodiesel yields approximately 1 kg of crude glycerol), and consequently this increase in production could create a surplus of crude glycerol that might not be absorbed by its current market [1].

The accumulation of crude glycerol may not only hamper the development of the biodiesel industry, but may also create both economic and environmental problems. In this context, various processes are being investigated in order to upgrade this biodiesel-derived glycerol and thus improve the biodiesel economy and sustainability [2, 3]. A promising strategy is catalytic steam reforming, a catalytic process that allows the conversion of this biodiesel by-product into a hydrogen rich gas [4]. The valorisation of glycerol by catalytic steam reforming offers several advantages. It allows the generation of syngas and/or H_2 from this renewable material, which can consequently help to improve the economy of the biodiesel production process. Moreover, the hydrogen obtained can be used in other processes. Depending on the reaction conditions and the catalyst used, different chemicals such as methanol, other alcohols and aldehydes could be produced from this H_2 rich gas in a third generation bio-refinery [5]. In addition, a high purity H_2 can be obtained making use of the innovative continuous sorption-enhanced steam reforming concept developed by Dou et al. [6, 7], which not only

allows the production of high purity H_2 but also permits the regeneration of the sorbent and catalyst in the same process.

The catalytic steam reforming of glycerol has been studied in many works. However, as reviewed by Lin [3], these works were focused on understanding the effect of the operating conditions and the catalyst type during the reforming of reagent-grade glycerol. Ni based catalysts have been commonly used in this process since they meet the challenge of being active and selective towards H_2, although they are susceptible to deactivation by coking. Therefore, they are modified with different active phase and support modifiers to enhance the steam reforming and WGS reaction as well as increasing their attrition resistance [8-13].

Nevertheless, the glycerol discharged from biodiesel production plants consists not only of pure glycerol but also of many other chemicals [1]. The presence of these impurities in biodiesel-derived glycerol can significantly affect the catalytic steam reforming process.

There are few works studying the catalytic steam reforming of crude glycerol [4, 14-18]. The crude glycerol used in these works was made up of a mixture of glycerol, methanol, inorganic salts, polyglycerols and fatty acid impurities. In some of these works, the results obtained with reagent grade glycerol and crude glycerol were compared [4, 17].

Slinn et al. [4] studied and optimised the steam reforming of glycerol using a Pt-Al_2O_3 catalyst. They found optimum conditions for glycerol reforming at 860 °C, feeding 0.12

mol/min glycerol per kg of catalyst and employing a S/C ratio of 2.5 mol H_2O/mol C. Under these reaction conditions, a comparison between crude and reagent grade glycerol was established. It was found that the conversions and yields with crude glycerol were 70% of those obtained with pure glycerol. They reported that the long chain fatty acid impurities were harder to reform and more likely to form carbon.

Dou et al. [16] analysed the catalytic steam reforming of glycerol/crude glycerol with/without CO_2 sorption. The crude glycerol consisted of 70-90 wt.% glycerol, a methanol content lower than 15 wt.% and some FAMES: linoleic, palmitic, oleic and stearic acid methyl esters. The glycerol conversion and the composition of the gas obtained during the steam reforming were studied and compared at different temperatures. The crude glycerol conversions were 71%, 96%, and 100% at 400 °C, 500 °C, and 600 °C respectively. They were slightly higher than those of the pure glycerol under the same reaction conditions (63%, 92%, and 97%). It was suggested that the presence of thermally resistant residues was responsible for these differences. The H_2 content using crude glycerol was slightly higher than using pure glycerol (67-68 vol.% compared to 65-66 vol.%). It was concluded that the presence of methanol and FAMEs increased the H_2 content compared to that of the pure glycerol due to stoichiometry.

In the work of Valliyappan et al. [19] the results obtained with a synthetic crude glycerol solution made up of 60 wt.% of glycerol, 31 wt.% of methanol, 7.5 wt.% of water and 1.5 wt.% of potassium hydroxide were compared with those obtained employing pure glycerol at 800 ºC. In the absence of catalyst, a higher yield to gas (94% v.s 91%) and a lower yield to solid (7% v.s 9%) were reported for pure glycerol

than for crude glycerol, respectively. These differences were attributed to the deposition of KOH in the reactor, which helped to increase char formation. As regards gas composition, few differences between the crude and pure glycerol were found. In the presence of catalyst, the production of hydrogen and the yield to gas from crude glycerol were higher than those from pure glycerol, while the formation of char was higher for crude glycerol. The authors reported that the presence of potassium hydroxide in the glycerol solution could favour the gasification reactions and char formation.

The comparisons between crude and reagent grade glycerol show that higher coke contents were obtained when crude glycerol was used and indicate that the presence of fatty acid methyl esters in crude glycerol was one of the reasons. However, these global comparisons show contradictory results in some cases. Additionally, they do not show the individual effect of each of the most representative biodiesel-derived impurities on the process, that is to say, the rest of the alcohol and catalyst employed during the transesterification reaction (methanol and potassium hydroxide, respectively) as well as the possible effect of the presence of an acid. Sulphuric acid, phosphoric acid or acetic acid, among others, can be present in the glycerol solution if it is neutralised [1, 20].

Taking this information into account, the objective of this work is to study the effect of the presence of acetic acid, potassium hydroxide and methanol during the reforming of glycerol. Acetic acid is an organic acid that can be used in glycerol neutralisation without poisoning the catalysts that are habitually used in steam reforming. Potassium hydroxide is commonly employed as a homogeneous catalyst in biodiesel production. Methanol is an alcohol generally used in biodiesel production as well as during the

glycerol purification step [21]. Specifically, instead of a global comparison between crude and reagent grade glycerol, this work provides information about the effect of the presence in a glycerol/water solution of the three impurities considered alone and all the binary and ternary combinations of these impurities in different proportions.

The effect of these impurities on the catalytic steam reforming of glycerol has been studied theoretically and experimentally. In the theoretical study, the presence of acetic acid and methanol in the glycerol solution has been evaluated at temperatures between 400 and 700 ºC using the Gibbs energy minimization method. In the experimental study, the effect of the presence of acetic acid, methanol and potassium hydroxide in the glycerol solution has been investigated in a fluidised bed reactor at 550 ºC using a Ni-based catalyst. The product distribution and the compositions of the gas and liquid phases have been analysed.

2 Materials and methods

2.1 Theoretical study

The effect of the presence in a 30 wt.% glycerol aqueous solution of up to 3 wt.% of CH_3COOH and up to 5 wt.% of CH_3OH on the equilibrium gas composition at temperatures between 400 and 700 ºC has been theoretically evaluated. For this purpose, different simulations were conducted based on a 2 level (upper and lower), 3 factor (temperature, wt.% CH_3COOH and wt.% CH_3OH) Box-Wilson Central Composite Face Centred (CCF, α: ± 1) design of experiments. In each simulation, the gas composition (vol.% of each gas) was calculated using the Gibbs energy minimisation method employing three different thermodynamic packages (PRSV, Twu-

Sim-Tasonee and Lee-Kesler-Plöcker) and using Hysys 8.3 simulation software. The results were analysed by means of an ANOVA test with 95% confidence. The relative influence of the temperature and the concentrations of CH_3OH and CH_3COOH were calculated using the cause-effect Pareto Principle.

2.2 Experimental study

The influence of the presence of up to 5 wt.% of CH_3OH, 3 wt.% of CH_3COOH and 2.8 wt.% of KOH in a 30 wt.% glycerol/water solution has been experimentally investigated. The experiments were carried out in a fluidised bed reactor for 3 h at 550 ºC and atmospheric pressure using a coprecipitated Ni-Co/Al-Mg catalyst. The detailed preparation procedure of the catalyst and its characterisation results can be found in our previous communications [9, 11]. A spatial time defined as the mass of catalyst/mass flow rate of glycerol ($W/m_{glycerol}$) ratio of 15 g catalyst min/g glycerol and a u/u_{mf} ratio of 6 defined as the ratio between the superficial gas velocity and the velocity of the theoretically calculated minimum fluidisation [22] were employed in all the experiments. N_2 was used as a fluidising agent as well as an internal standard for the analysis of the gas phase.

A detailed description of the fluidised bed installation can be found in our previous communication [11]. However, for this work, a tubular 2.54 cm inner diameter stainless steel fluidised bed reactor was used instead of the original quartz reactor due to the presence of KOH in some of the solutions. In addition, the condensation system was also modified. Three condensers were used in this work to collect the liquid condensates at intervals of 60 minutes in order to study the evolution over time of the liquid phase.

To study the effect of the presence of the individual impurities as well as the effect of all the possible binary and ternary combinations of the impurities (2 or 3 impurities), the experiments were designed using a 2^k factorial design, where k indicates the number of factors studied (in this case 3 impurities) and 2^k represents the number of runs (in this case 8). In addition, three replicates at the centre point (centre of the variation interval of each factor) were carried out in order to evaluate both the experimental error and the curvature shown by the evolution of each variable, i.e. whether or not this evolution is linear within the experimental range studied.

2.3 Data analysis

First of all, the evolution over time was studied. For each experiment, the results are divided into three intervals. Each interval corresponds to the average value of the studied response variables obtained during the first, second and third hour of the experiment. All these values (three per experiment) have been compared using a one-way analysis of variance (one-way ANOVA) and Fisher´s least significant difference (LSD) test, both with 95% confidence. The results of the ANOVA analyses are provided as p-values. P-values lower than 0.05 indicate that at least two values are significantly different. Furthermore, the LSD test was used to compare pairs of data, i.e. either between two intervals of the same experiment or between two intervals of two different experiments. The results of the LSD tests are presented graphically in the form of LSD bars. To ensure significant differences between any pair of data, their LSD bars must not overlap.

Secondly, the effect of the impurities was studied considering the results corresponding to the first hour using a statistical analysis of variance (one-way ANOVA) test with

95% confidence. This strategy allows not including the effect of the variations with time of the different response variables in the analysis. The ANOVA analyses evaluate whether the effect of the impurities, their interactions and the curvature have a significant influence or not on the response variables. In addition, the cause-effect Pareto Principle was also used to calculate their relative importance.

The response variables studied are: global glycerol conversion (X gly), carbon conversion to gases, liquids and solid products (CC gas, CC liq and CC sol) as well as the composition of the gas (N_2 and H_2O free, vol.%) and liquid (relative chromatographic area free of water and un-reacted glycerol, %). The CC sol was calculated by difference and includes both the carbon deposited on the catalyst (coke) and the carbon resulting from an incomplete vaporisation of the feed (char). The used catalyst was characterised by elemental analysis to calculate the amount of carbon deposited on the catalyst surface. The CC coke and the amount of C deposited with respect to the amount of catalyst and organics (glycerol, acetic acid and methanol) reacted (mg C/g catalyst g organics reacted) were calculated from these analyses. CC char was therefore calculated by difference. Table 1 summarises the response variables and the analytical methods used for their calculation.

In the simulations made for the theoretical study and the fluidised bed experiments, the lower and upper limits of all the factors (temperature and concentration of CH_3COOH and CH_3OH for the theoretical study and the concentration of CH_3COOH, CH_3OH and KOH for the experimental investigation) were normalised from -1 to 1 (codec factors).

This codification permits that all factors vary within the same interval and helps to investigate their influence in comparable terms.

3. Results and discussion

3.1 Thermodynamic results

Table 2 shows the temperature and the concentrations of each impurity in the 30 wt.% glycerol aqueous solutions employed in the simulations. The equilibrium volumetric compositions obtained for each simulation, expressed as the 95% confidence interval for the mean obtained with the three thermodynamic packages of each mixture, are also presented in Table 2. The thermodynamic results predict a 100% glycerol conversion into gases within the whole range of temperatures studied in this work. The gases comprise H_2, CO_2, CO and CH_4. Depending on the temperature and the concentration of CH_3COOH and CH_3OH, the gas composition varies as follows: 46-70 vol.% H_2, 21-33 vol.% CO_2, 0.73-12 vol.% CO and 0.03-21 vol.% CH_4. The thermodynamic formation of solid C is considered negligible under the operating conditions employed, which is in accordance with the results of other thermodynamic studies [23-27].

The results of the ANOVA and Pareto Principle analyses are shown in Table 3. This table reveals that the temperature (including linear and quadratic terms) is the factor with the highest influence on the thermodynamic gas composition, having 84% importance for the relative amount of H_2 and CH_4, 81% for the CO_2 and 77% for the CO. The presence of up to 3 and 5 wt.% of CH_3COOH or CH_3OH, respectively, has a significant influence (p-values < 0.05 in the ANOVA analysis) on the thermodynamic

gas composition. However, their relative importance is very low from a practical point of view, being lower than 10% according to the Pareto analysis.

These results are in agreement with those published by Hajjaji et al. [28] where the effect of the temperature and the steam to carbon (S/C) ratio (mol/mol) on the thermodynamics of the autothermal reforming of crude glycerol was theoretically investigated. Furthermore, they are also consistent with the results reported by Silva et al. [26], who studied the effect of the temperature and the molar water/glycerol feed ratio (WGFR) on the thermodynamic results of glycerol steam reforming. Both studies reported that the reforming temperature exerts a greater impact than the S/C ratio or the WGFR on the thermodynamic results.

Furthermore, in this work the variation interval for the temperature (400-700 ºC) is higher than that for the S/C ratio. A 30 wt.% glycerol water solution without impurities has a S/C ratio of 3.98, which decreases as the concentration of impurities in the solution increases, reaching its lowest value (2.79) for a 30 wt.% glycerol solution having 5 wt.% of CH_3OH and 3 wt.% of CH_3COOH.

Fig. 1 shows the volumetric composition of the gas obtained during the reforming of a 30 wt.% glycerol solution, as well as the volumetric gas composition for two 30 wt.% glycerol solutions, one having 3 wt.% of CH_3COOH and the other 5 wt.% of CH_3OH, predicted from the empirical models calculated from the ANOVA analysis. Since a quadratic model was used, a negative concentration of CH_4 is predicted at temperatures higher than 600 ºC, instead of the real asymptotic evolution.

Regarding the effect of the temperature, an increase from 400 to 700 ºC augments the relative amount of H_2 and CO in all cases due to the endothermic nature of the steam reforming of glycerol [3], acetic acid [29] and methanol [30] (Eqs.1-3). In addition, the water gas shift (WGS) reaction (Eq.4) is exothermic [29], therefore the relative amount of CO in the gas increases as the temperature increases. Conversely, this increase in temperature reduces the concentration of CO_2 and CH_4 in the gas due to the exothermic nature of the WGS and methanation reactions (Eq.5), as well as the endothermicity of the methane reforming reaction (Eq.6) [28]. An optimum temperature for H_2 production is found at temperatures around 580-610ºC, which is in agreement with those reported by other authors [21, 26, 31, 32].

$$C_3H_8O_3 + 3\ H_2O \rightarrow 7\ H_2 + 3\ CO_2 \quad \text{(Eq.1)}$$

$$CH_3OH + H_2O \rightarrow 3\ H_2 + CO_2 \quad \text{(Eq.2)}$$

$$CH_3COOH + 2\ H_2O \rightarrow 4\ H_2 + 2\ CO_2 \quad \text{(Eq.3)}$$

$$CO + H_2O \Leftrightarrow H_2 + CO_2 \quad \text{(Eq.4)}$$

$$CO + 3\ H_2 \Leftrightarrow CH_4 + H_2O \quad \text{(Eq.5)}$$

$$CH_4 + H_2O \Leftrightarrow 4\ H_2 + CO_2 \quad \text{(Eq.6)}$$

The presence of the impurities slightly changes the composition of the gas, as was predicted by the Pareto test, and their effect depends on the reforming temperature. At temperatures lower than 500 ºC, the addition of up to 3 wt.% of CH_3COOH or 5 wt.% of CH_3OH to the 30 wt.% glycerol solution diminishes the concentration of H_2, increasing the concentration of CO and CH_4. The addition of CH_3COOH increases the proportion of CO_2, while the addition of CH_3OH decreases it.

At temperatures higher than 500 ºC, the effect of the impurities is slightly different. A decrease in the concentration of CO_2 together with an increase in the concentration of CO is observed when the glycerol solution contains either CH_3OH or CH_3COOH. The addition of up to 3 wt.% of CH_3OH to the glycerol solution has a negligible effect on the concentration of H_2, while the addition of CH_3COOH decreases the proportion of H_2 in the gas. The relative amount of CH_4 in the gas increases with the addition of both impurities. At temperatures higher than 600 ºC the effect of the impurities is not significant and the proportion of CH_4 in the gas drops to zero in all cases.

These results are the consequence of two factors, the stoichiometry of the reforming reactions and the S/C ratio of the solutions, which depend on the concentration of the impurities. According to their stoichiometry, the steam reforming of glycerol, methanol and acetic acid (Eqs. 1-3) gives 2.33 mol H_2/mol C, 3 mol H_2/mol C and 2 mol H_2/mol C, respectively. The S/C ratios for a 30 wt.% glycerol solution without impurities and for two 30 wt.% glycerol solutions having 3 wt.% of CH_3COOH or 5 wt.% of CH_3OH are 3.98, 3.45 and 3.18, respectively.

At temperatures lower than 500 ºC the methane reforming reaction is not favoured due to its endothermic nature, and the gas contains a high concentration of CH_4. In this case the proportion of CH_4 in the gas also depends on the S/C ratio of the solution. The lower the S/C ratio, the lower the reforming of methane. Consequently, the proportion of CH_4 in the gas increases as the S/C of the different solutions decreases. This trend also applies for the proportion of CO in the gas. The lower the S/C ratio, the lesser the shift of the WGS reaction towards the production of H_2 and CO_2 and, consequently, the higher the proportion of CO in the gas.

This decrease in the S/C ratio also causes a lower proportion of H_2 in the gas when either CH_3OH or CH_3COOH are added to the solution. The lower the S/C ratio, the higher the proportion of CH_4 and the lower the concentration of H_2 in the gas, since the reforming reaction towards H_2 is not favoured at low temperatures. However, the stoichiometry also influences the proportion of H_2. As a result, the same proportion of H_2 in the gas is obtained with solutions containing 30 wt.% of glycerol with 3 wt.% of CH_3COOH or 5 wt.% of CH_3OH at temperatures lower than 500 ºC.

A decrease in the proportion of CO_2 is noticed when a 5 wt.% of CH_3OH is added to the solution, due to the increase in the concentration of CH_4. The addition of 3 wt.% of CH_3COOH slightly increases the proportion of CO_2. In this case, the drop in the concentration of H_2 is not compensated for by the increase in the concentration of CH_4.

At temperatures higher than 500 ºC, the proportion of CH_4 in the gas becomes negligible and consequently the impurities do not exert any influence on the proportion of this gas. However, the WGS reaction, due to its exothermic nature, has a lesser tendency towards the production of H_2 and CO_2. Consequently, the effect of the S/C ratio exerts a greater influence on the proportion of CO at high than at low temperatures. This provokes a greater increase in the proportion of CO together with a decrease in the concentration of CO_2 with the decrease in the S/C ratio.

In contrast, the effect of the S/C ratio is less important than the effect of the stoichiometry for the relative amount of H_2 in the gas, since at high temperatures the reforming process is favoured. Consequently, the variations in the concentration of H_2

in the gas are mainly related to stoichiometry. The concentration of H_2 slightly increases when the 30 wt.% glycerol solution contains 5 wt.% of CH_3OH and decreases when it contains 3 wt.% of acetic acid (Eqs. 1-3).

3.2 Experimental results

From the theoretical study an optimum temperature for H_2 production can be found at temperatures around 580-610 ºC. However, the catalytic steam reforming experiments were carried out at 550 ºC. This slightly lower temperature was chosen having regard to the energetic aspects of the process, as well as aiming to have a gas made up of all the gases considered, H_2, CO_2, CO and CH_4, in order to study the increases and decreases in their concentrations with the presence of the impurities. Table 4 shows the composition (in actual and codec factors), the S/C ratio and the pH of the 30 wt.% glycerol solutions employed in the experiments according to the 2^k design.

3.2.1 Glycerol conversion and carbon distribution (CC gas, CC liq and CC sol)

A complete glycerol conversion (X gly = 100%) is achieved for all the experiments, indicating that all the glycerol was converted into gas, liquid and solid products. Fig. 2 shows the CC gas, CC liq and CC sol obtained for the different experiments represented in three intervals of 1 hour. The ANOVA analyses revealed statistically significant differences for the CC gas (p-value = 0.01), CC liq (p-value = 0.025) and CC sol (p-value = 0.012) obtained in the experiments. Specifically, the CC gas, CC liq and CC sol varied as follows: 75-100%, 0-2.5% and 0-25%, respectively.

As regards the temporal evolution, an increase in the CC gas over time together with a decrease for the CC sol are detected for the experiments containing KOH (runs 5, 8 and

9-11). The presence of KOH in the solutions might hinder the evaporation of the other organic compounds in the feed, leading to low initial (1st h) CC gas and high CC sol. Inorganic salts in a water solution decrease the evaporation rate of the other organic compounds [33], which might result in a higher formation of carbonaceous deposits (char) [34]. However, as the reaction advances and KOH progressively accumulates inside the reactor, their presence exerts a positive catalytic effect [35, 36], aiding the gasification of these carbon deposits. The accumulation of salts in the catalyst bed was also reported in the work of Fermoso et al. [17]. They observed NaOH in the upper part of the bed when using a fixed bed reactor for the reforming of crude glycerol where NaOH had been employed in the transesterification step.

The feed solutions for runs 6 and 7 also contain KOH. However, the increase in the CC gas over time did not take place. These solutions contain CH_3COOH or CH_3OH, which can transform KOH into CH_3COOK, a colourless liquid at standard temperature and pressure, or into CH_3OK, a white to yellow hydroscopic powder that decomposes at temperatures higher than 50 ºC, respectively [37]. The interaction between impurities can explain the results observed for runs 6 and 7. Additionally, the complete elimination of KOH is not possible for runs 8 and 9-11 due to the different amounts of impurities, and consequently an increase in the CC gas over time is observed. These interactions between impurities will be further discussed for the results obtained during the first hour of reaction, making use of a statistical analysis.

Decreases in the CC gas along with increases in the CC liq with time are also detected. These trends are noticeable for runs 1, 2 and 6, where the CC liq slightly increases with

time, suggesting a small catalyst deactivation. This deactivation is not severe and the corresponding decrease in the CC gas is only noticeable in experiment 1.

To study the specific effect of the impurities as well as their possible interactions on the catalytic steam reforming of glycerol, the results obtained during the first hour of each experiment have been statistically analysed and compared. The results of these analyses are summarised in Table 5 and Fig. 3, where the most important interactions between the impurities are shown.

The ANOVA analysis reveals that the presence of CH_3COOH, CH_3OH and KOH in the 30 wt.% glycerol solutions has a significant influence on the CC gas and CC sol obtained during the first hour. Furthermore, significant interactions between impurities are also detected. The analysis of the curvature for the CC gas and CC sol shows a linear trend for both variables within the studied range with 95% confidence (p-value < 0.05). In contrast, the impurities do not exert any significant influence on the CC liq during the first hour and the CC liq is lower than 1.5% in all the experiments. Thus, the possible effect of CH_3COOH and CH_3OH on the glycerol reforming pathway is considered negligible under the operating conditions employed. The effect on the reforming results of all the different glycerol/impurity mixtures is discussed below in sections 3.2.1.1-3.2.1.3, making use of the statistical analyses of the results.

3.2.1.1 Effect of one impurity

As regards the presence of only one impurity, the ANOVA analysis (positive or negative coefficients in the model) indicates that the presence in the glycerol solution of CH_3COOH and KOH provokes a decrease in the CC gas along with an increase in the

CC sol, while the presence of CH_3OH exerts the opposite effect. The Pareto analysis reveals that the impurities with the highest influence on these results are the KOH (28%) and CH_3OH (27-28%), followed by CH_3COOH (15%).

Fig. 3 shows the effect of each impurity as well as the binary and ternary mixtures on the CC gas and CC sol. As regards the presence of only one impurity, it can be seen that up to 5 wt.% of CH_3OH can be added to the glycerol solution without exerting any statistically significant influence on either the CC gas or the CC sol. CH_3OH is very reactive in the reforming process and has a low tendency to char formation thanks to its low boiling point and molecular mass. This negligible effect of CH_3OH has also been reported in the catalytic gasification of a simulated crude glycerol solution having CH_3OH and KOH as impurities [19].

Conversely, the progressive addition of up to 2.8 wt.% of KOH to the solution diminishes the CC gas from 95% to 76%, and increases the CC sol from 3 to 22%. As previously remarked, inorganic salts decrease the evaporation rate of the other organic compounds [33], leading to a higher formation of carbonaceous deposits [34].

The effect of the addition of up to 3 wt.% CH_3COOH to the glycerol solution can be gathered comparing Fig. 3a with Fig. 3b (for the CC gas) and Fig. 3c with Fig. 3d (for the CC sol). This comparison shows how the CC gas decreases from 95 to 86% and the CC sol increases from 3 to 13%. The addition of CH_3COOH to the glycerol solution might lead to the formation of different esterification products [38], such as glyceryl monoacetate (Eq.7), glyceryl diacetate (Eq.8) and glyceryl triacetate (Eq.9). These reactions can occur during the preparation of the solutions and/or during the feeding of

the solution into the reactor, where these reactions can be intensified thanks to the temperature of the feeding system (70 ºC). The presence of small amounts of these compounds in some of the liquid condensates supports this hypothesis.

$C_3H_8O_3 + CH_3COOH \rightarrow C_3H_7O_2(CH_3COO)$ (Eq.7)

$C_3H_7O_2(CH_3COO) + CH_3COOH \rightarrow C_3H_6O(CH_3COO)_2$ (Eq.8)

$C_3H_6O(CH_3COO)_2 + CH_3COOH \rightarrow CH_3H_5(CH_3COO)_3$ (Eq.9)

The formation of these compounds, therefore, might increase the formation of carbonaceous deposits due to their relatively high molecular mass. An increase in the molecular mass leads to bigger droplet sizes, causing the evaporation of the feed to take place at lower heating rates, increasing the CC sol [34].

3.2.1.1 Effect of two impurities

In relation to the binary combinations (KOH-CH_3OH, KOH-CH_3COOH and CH_3OH-CH_3COOH), it is worth mentioning that the effect of the presence of KOH is different when it is alone or accompanied by CH_3COOH than when it is accompanied by CH_3OH. Figs. 3a and 3c show how the progressive addition of CH_3OH to a glycerol solution having 2.8 wt.% of KOH reduces the negative effect of the KOH, i.e. it increases and decreases the CC gas and CC sol, respectively. These results can be explained by the progressive removal of KOH and its transformation into CH_3OK (Eq.10), decreasing the negative effect that KOH exerts on the evaporation of the other organic compounds in the feed.

$CH_3OH + KOH \rightarrow CH_3OK + H_2O$ (Eq. 10)

CH_3OK decomposes at temperatures higher than 50 ºC [37] and the effect of having a solid compound in the solution disappears. This confirms the fact that some inorganic salts decrease the evaporation rates of organic compounds [33].

Conversely, the effect of the addition of CH_3COOH to a glycerol solution containing 2.8 wt.% of KOH does not exert any effect on either the CC gas or the CC sol, as can be gathered comparing Fig 3.a with 3b and Fig 3.c with d, respectively. According to Eq. 11, when CH_3COOH is added to the solution, part of the acid can be progressively transformed into CH_3COOK, a colourless liquid at standard temperature and pressure [37], creating a CH_3COOH/CH_3COO^- buffer solution.

$$KOH + CH_3COOH \rightarrow CH_3COOK \qquad \text{(Eq.11)}$$

In this case, glyceryl acetates can also be produced from the reaction of glycerol with either CH_3COOH and/or CH_3COOK, and a decrease in the CC gas and an increase in the CC sol are experimentally observed. In addition, since the same molar concentration of CH_3COOH and KOH are present in the solution when the highest amounts of these two impurities are considered, the complete removal of KOH might not be possible. The presence of KOH in the solution, as explained above, also provokes a decrease and an increase in the CC gas and CC sol, respectively. Furthermore, Fig. 3b and 3d illustrate how the addition of 2.8 wt.% of KOH to a glycerol solution containing 3 wt.% of CH_3COOH enhances the negative effect of the acid. This suggests that either the complete removal of KOH is not possible or the formation of glyceryl acetates from

glycerol could be more favoured with CH_3COOK than with CH_3COOH, probably due to its higher basic character.

Additionally, although experimentally KOH and CH_3COOK exert the same effect on the initial results, their presence in the solution does not have the same consequences for the evolution over time of the CC gas and CC sol. Fig.2 shows how the progressive accumulation of KOH in the reactor progressively increases the CC gas with time thanks to its catalytic effect on char gasification (run 5). However, in run 6 (CH_3COOH and KOH) this catalytic effect is not observed, which indicates a decrease in the concentration of KOH in the solution.

As regards the presence of CH_3COOH and CH_3OH in the glycerol solution, Figs. 3b and 3d show how the negative effect of CH_3COOH on the CC gas is reduced as the amount of CH_3OH in the solution progressively increases as a result of the plausible esterification reaction between the two impurities (Eq. 12).

$$CH_3COOH + CH_3OH \rightarrow CH_3COOCH_3 + H_2O \qquad \text{(Eq. 12)}$$

These results seem to indicate that the presence in the solution of CH_3COOCH_3, a colourless liquid with a relatively low normal boiling point (57 ºC) [37], does not favour the formation of carbonaceous deposits from the feed.

3.2.1.3 Effect of the three impurities

Figs. 3 b and d show the effect of the presence of the three impurities on the CC gas and CC sol, respectively. It is observed how the addition of KOH to a glycerol solution

containing 3 wt.% of CH_3COOH results in a reduction of the CC gas and an increase in the CC sol regardless of the concentration of CH_3OH present in the solution. As the concentration of CH_3OH in the solution increases, the CC gas increases and the CC sol decreases. However, in the presence of the three impurities the positive effect of the addition of CH_3OH does not produce as much CC gas as that obtained in the absence of KOH. The CC gas is higher for the binary CH_3COOH-CH_3OH mixture than for the ternary CH_3COOH-CH_3OH-KOH mixture. In addition, in the presence of CH_3COOH, the positive effect of CH_3OH in compensating for the negative effect of KOH is also reduced. Consequently, the CC gas for the ternary CH_3COOH-CH_3OH-KOH mixture is lower than that for the binary mixture KOH-CH_3OH.

When the three impurities are present in the glycerol solution, different reactions (Eqs. 10-13) can take place depending on the concentration of the impurities.

$$CH_3COOK + CH_3OH \rightarrow CH_3COOCH_3 + KOH \qquad \text{(Eq.13)}$$

When the glycerol solution contains the maximum amount of the three impurities considered in this work, according to Eqs.10-13 the negative effect of the formation of CH_3COOK is reduced as the concentration of CH_3OH increases to its highest value. This can be seen in Figs. 3 b and d. However, the addition of CH_3OH also leads to the formation KOH (Eq. 13). This suggests that in the ternary mixture with the highest amounts of all the impurities, the KOH is not completely removed. This result is in agreement with that experimentally observed when analysing the evolution of the CC gas and CC sol over time (Fig. 2). Run 8 refers to the reforming of a glycerol solution containing the highest amount of impurities, and relatively little CC gas is obtained.

This CC gas is lower than the amount obtained in the absence of impurities but higher than that obtained with the highest amount of KOH. In addition, an increase in the CC gas along with a decrease in the CC sol over time is also observed, which suggests that KOH is still present in the solution.

3.2.2 Overall carbon distribution

To corroborate the relationship observed between the CC gas and CC sol, a multivariate analysis by means of Spearman´s test was carried out for the CC gas, CC sol and CC liq obtained in all the experiments, including the three values per experiment. A statistically significant and high relationship (p-value = 0.0001; $R^2 = 0.96$) was found between the CC gas and CC sol. This confirms that the low CC gas is a result of high CC sol due to the formation of carbon deposits that diminish the amount of C in the gas phase.

Additionally, to distinguish between the carbon deposited on the catalyst (coke) and the carbonaceous deposits originated from an incomplete vaporisation of the feed (char), the used catalysts were characterised by elemental analysis. Table 6 shows the 3-hour overall carbon distribution (CC sol, CC char and CC coke) as well as the carbon deposited on the catalyst expressed as mg C/ g catalyst g organics reacted [39] obtained for all the experiments. These values were compared between the different experiments using an ANOVA analysis with 95% confidence and are also presented in Table 6.

The CC coke and C deposited on the catalyst are lower than 0.82% and 1.13 mg C/g catalyst g org reacted, respectively. These values suggest a low catalyst deactivation. As an example, in a previous work where this catalyst was used for the catalytic reforming

of the aqueous fraction of bio-oil in a fluidised bed [11], both CC gas and gas composition were reported steady over time with an amount of C deposited on the catalyst (10 mg C/ g catalyst g organic reacted) higher than that obtained in this work. Moreover, analysing the C distribution obtained in the present work, more than 80% of the total solid C is due to char formation, indicating that the vast majority of the CC sol is due to the formation of char.

3.2.3 Gas composition

Fig. 4 shows the gas composition obtained for the different experiments. The impurities have a statistically significant influence on the relative amount of H_2 (p-value = 0.003), CO_2 (p-value = 0.002), CO (p-value = 0.001) and CH_4 (p-value = 0.006). The relative amount (vol.%) of H_2, CO_2, CO and CH_4 varied from 66-70%, 24-29%, 3-6% and 0.5-2.5%. These small variations are in agreement with those reported in works comparing reforming results obtained with crude and reagent grade glycerol [4, 16, 19, 32].

Studying the evolution of the gas over time, the general tendency shows small variations. This indicates a low catalyst deactivation, which is in agreement with the low values obtained for the CC coke and the small amounts of C (mg C/g catalyst g org) quantified in the used catalysts. One exception is run 5, which contains KOH, and where a decrease in the proportion of H_2 along with increases in the concentrations of CO and CH_4 take place. Moreover, in this run a substantial increase in the CC gas over time is noticed, which could be the consequence of the progressive gasification of carbon deposits (Eqs. 14-16), augmenting the proportion of C in the gas.

$C + H_2O \Leftrightarrow CO + H_2$ (Eq. 14)

$C + 2\ H_2 \Leftrightarrow CH_4$ (Eq. 15)

$C + CO_2 \Leftrightarrow 2\ CO$ (Eq. 16)

The results obtained during the first hour of experiment have been statistically analysed and compared making use of an ANOVA test with 95% confidence. Table 7 shows the relative influence of the impurities on the gas composition (Pareto analysis) as well as their positive or negative effect (terms in the codec model).

The concentration of H_2 and CO_2 during the first hour of experiment ranges from 67.0 to 69.8 vol.%, and from 24.5 to 27.15 vol.%, respectively. These small variations indicate that the effect of the impurities on these variables is small. According to Table 7, the impurity with the highest influence on the proportion of H_2 is CH_3COOH (24%), followed by CH_3OH (17%) and KOH (13%), while for the relative amount of CO_2, CH_3OH and CH_3COOH, with 28% and 15% influence respectively, are the impurities with the highest influence. The concentrations of CO and CH_4 in the gas are little affected by the presence of the impurities; there are small variations in the proportions of these two gases. CH_3OH is the only impurity affecting the proportion of CO. The relative amount of CH_4 was affected by the presence of CH_3COOH (22%) and CH_3OH (61%).

The variations in the composition of the gas in the presence of the impurities can have a thermodynamic and/or kinetic background. The thermodynamic and experimental gas compositions can be compared by looking at Tables 3 and 7. The experiments were carried out at 550 ºC, which corresponds to a codec value of zero for the temperature in the thermodynamic model as it is the centre of the variation of the temperature.

Consequently, at 550 ºC the experimental and thermodynamic terms for the concentrations of CH_3OH and CH_3COOH in the thermodynamic and experimental models can be directly compared.

The comparison between the independent terms of Table 3 and Table 7 provides a direct comparison between the thermodynamic and experimental results of a 30 wt.% glycerol solution having 1.5 wt.% of CH_3COOH, 2.5 % of CH_3OH and 1.4 wt.% of KOH. The concentrations of these impurities in a 30 wt.% glycerol solution are very similar to the values obtained when the biodiesel derived-glycerol is neutralised with CH_3COOH and refined with a vacuum distillation to recover CH_3OH and CH_3COOH [1, 20]. This comparison shows that the experimental gas compositions are very similar to the thermodynamically predicted compositions. A slightly higher concentration of H_2 and lower concentrations of CO and CH_4 are obtained experimentally. These small differences could be due to the formation of carbonaceous deposits, the majority as char.

As regards the effect of the presence of the impurities in the glycerol solution, the small values of the coefficients for their concentrations in Tables 3 and 7 confirm the small variations caused by the impurities on the thermodynamic and experimental gas compositions.

The coefficient for CH_3COOH in Table 7 shows how its presence alone in the glycerol solution increases the concentrations of CO_2 and CH_4 in the gas and reduces the proportion of H_2, while the concentration of CO is unaffected. The decrease in the proportion of H_2 and the increase in CH_4 are thermodynamically predicted (Table 3). In

addition, the similar values for their coefficients in the thermodynamic and experimental models suggest that the variations can be thermodynamically explained. However, the increase in the proportion of CO_2 must have a kinetic origin, perhaps related to the decomposition of CH_3COOH into CO_2 [40].

The presence of CH_3OH as the only impurity increases the concentrations of CO and CH_4 in the gas, decreasing the proportion of H_2 and CO_2. The increases in CO and CH_4 are thermodynamically predicted and the similar values for their coefficients in the thermodynamic and experimental models suggest a thermodynamic origin for these two variations. However, the variations observed for H_2 and CO_2 are not wholly predicted by the thermodynamics. The decrease in the proportion of H_2 is higher in the experimental model than the thermodynamic model while the decrease in the CO_2 is lower. The higher experimental decrease in the proportion of H_2 can be explained by the decrease in the S/C ratio and spatial time. The spatial time in carbon basis decreases from 460 g catalyst min/mol C (for a 30 wt.% glycerol solution) to 397 g catalyst min/mol C (for a 30 wt.% glycerol solution having 5 wt.% of CH_3OH). Thus the reforming and the water gas shift reactions do not generate the thermodynamically predicted hydrogen content.

An increase in the concentration of KOH leads to a gas with a higher concentration of H_2 and lower proportions of CO and CO_2. This might indicate that this impurity exerts a positive catalytic effect in the reforming process [35, 36]. Conversely, it does not exert any significant influence on the relative amount of CH_4, which might suggest that this impurity does not exert any noticeable catalytic effect on methane reforming under the operating conditions used in this work.

3.2.4 Liquid composition

The liquid phase was made up of a mixture of alcohols (methanol and ethanol), aldehydes (acetaldehyde), ketones (1-hydroxy-2-propanone, acetone), phenols (phenol, phenol-2methyl, phenol-3-methyl), cyclic compounds and small amounts of glyceryl acetates.

Fig. 5 shows the concentration of the most abundant families of compounds. The statistical analysis of the results shows that the impurities exert a statistically significant influence on the relative amount of aldehydes (p-value = 0.007), alcohols (p-value = 0.013), phenols (p-value = 0.003), ketones (p-value = 0.019), and cyclic compounds (p-value = 0.001). However, the low CC liq obtained in all the experiments must be taken into consideration (CC liq < 2.5 %).

The relative amount of aldehydes varies from 0 to 15% while alcohols vary from 0 to around 70%. The presence of methanol in the liquid may be the consequence of its presence in the feed and/or its production during glycerol reforming [3]. Phenols and cyclic compounds vary from 0-90% and 0-28%, respectively. A huge increase in these compounds can be seen when the glycerol solution only contains KOH. The presence of KOH might favour the formation of cyclic compounds during the reforming of glycerol, which is in agreement with the pathway proposed in the work of Lin [3]. The relative amount of ketones shifts from 0 to 90%. In addition, the proportion of ketones becomes negligible when KOH is the only impurity. These results suggest that when the glycerol solution has a high amount of KOH, a possible catalytic effect of this impurity on the glycerol condensation reaction with ketones might take place [41].

4. Conclusions

The effect has been studied of the presence in a 30 wt.% glycerol aqueous solution of up to 3 wt.% CH_3COOH, 2.8 wt.% KOH and 5 wt.% CH_3OH on the catalytic steam reforming process both theoretically and experimentally in a fluidised bed reactor at 550 ºC. The most significant conclusions are summarised as follows.

1. The theoretical study showed that the temperature is the factor with the highest influence on the thermodynamic results. The presence of the studied amounts of CH_3COOH and CH_3OH barely influences the thermodynamic composition of the gas.

2. The experimental results indicated that the carbon conversion to gas and solid are strongly affected by the presence of CH_3COOH, CH_3OH and KOH. Specifically, the CC gas and CC sol and vary from 75 to100 % and 0 to 25%, respectively. The carbon conversion to liquid varies from 0 to 2.5%. The composition of the gas is little affected by the presence of the impurities. In contrast, the impurities significantly affect the liquid composition.

3. Regarding the presence of the impurities alone, CH_3OH does not statistically influence the initial CC gas and CC sol. In contrast, CH_3COOH and KOH decrease the initial CC gas and increase the CC sol. However, when the glycerol solution contains KOH, its progressive accumulation inside the reactor exerts a positive catalytic effect on the gasification of the carbonaceous deposits, decreasing the CC sol over time.

4. When two or more impurities are present together in the glycerol solution, other reactions between the impurities such as neutralisation and esterification can occur prior to or during the reforming reactions, explaining the results observed in this work.

ACKNOWLEDGEMENTS

The authors wish to express their gratitude to the Spanish MINECO (projects ENE2010-18985 and ENE2013-41523-R) for providing financial support and the FPI grant awarded to Javier Remón Núñez (BES- 2011-044856).

REFERENCES

[1] R. Manosak, S. Limpattayanate, M. Hunsom, Sequential-refining of crude glycerol derived from waste used-oil methyl ester plant via a combined process of chemical and adsorption, Fuel Processing Technology, 92 (2011) 92-99.
[2] A. Corma, G. Huber, L. Sauvanaud, P. Oconnor, Biomass to chemicals: Catalytic conversion of glycerol/water mixtures into acrolein, reaction network, Journal of Catalysis, 257 (2008) 163-171.
[3] Y.-C. Lin, Catalytic valorization of glycerol to hydrogen and syngas, Int J Hydrogen Energy, 38 (2013) 2678-2700.
[4] M. Slinn, K. Kendall, C. Mallon, J. Andrews, Steam reforming of biodiesel by-product to make renewable hydrogen, Bioresource technology, 99 (2008) 5851-5858.
[5] X. Song, Z. Guo, Technologies for direct production of flexible H_2/CO synthesis gas, Energy Conversion and Management, 47 (2006) 560-569.
[6] B. Dou, Y. Song, C. Wang, H. Chen, M. Yang, Y. Xu, Hydrogen production by enhanced-sorption chemical looping steam reforming of glycerol in moving-bed reactors, Applied Energy, 130 (2014) 342-349.
[7] B. Dou, C. Wang, H. Chen, Y. Song, B. Xie, Continuous sorption-enhanced steam reforming of glycerol to high-purity hydrogen production, Int J Hydrogen Energy, 38 (2013) 11902-11909.
[8] B. Dou, C. Wang, Y. Song, H. Chen, Y. Xu, Activity of Ni–Cu–Al based catalyst for renewable hydrogen production from steam reforming of glycerol, Energy Conversion and Management, 78 (2014) 253-259.
[9] J. Remón, F. Broust, J. Valette, Y. Chhiti, I. Alava, A.R. Fernandez-Akarregi, J. Arauzo, L. Garcia, Production of a hydrogen-rich gas from fast pyrolysis bio-oils: Comparison between homogeneous and catalytic steam reforming routes, Int J Hydrogen Energy, 39 (2014) 171-182.

[10] J. Remón, F. Broust, G. Volle, L. García, J. Arauzo, Hydrogen production from pine and poplar bio-oils by catalytic steam reforming. Influence of the bio-oil composition on the process, Int J Hydrogen Energy, 40 (2015) 5593-5608.
[11] J. Remón, J.A. Medrano, F. Bimbela, L. García, J. Arauzo, Ni/Al–Mg–O solids modified with Co or Cu for the catalytic steam reforming of bio-oil, Applied Catalysis B: Environmental, 132-133 (2013) 433-444.
[12] C. Wang, B. Dou, H. Chen, Y. Song, Y. Xu, X. Du, T. Luo, C. Tan, Hydrogen production from steam reforming of glycerol by Ni–Mg–Al based catalysts in a fixed-bed reactor, Chemical Engineering Journal, 220 (2013) 133-142.
[13] C. Wang, B. Dou, H. Chen, Y. Song, Y. Xu, X. Du, L. Zhang, T. Luo, C. Tan, Renewable hydrogen production from steam reforming of glycerol by Ni–Cu–Al, Ni–Cu–Mg, Ni–Mg catalysts, Int J Hydrogen Energy, 38 (2013) 3562-3571.
[14] S. Authayanun, A. Arpornwichanop, W. Paengjuntuek, S. Assabumrungrat, Thermodynamic study of hydrogen production from crude glycerol autothermal reforming for fuel cell applications, Int J Hydrogen Energy, 35 (2010) 6617-6623.
[15] K.S. Avasthi, R.N. Reddy, S. Patel, Challenges in the Production of Hydrogen from Glycerol – A Biodiesel Byproduct Via Steam Reforming Process, Procedia Engineering, 51 (2013) 423-429.
[16] B. Dou, G.L. Rickett, V. Dupont, P.T. Williams, H. Chen, Y. Ding, M. Ghadiri, Steam reforming of crude glycerol with in situ CO_2 sorption, Bioresource technology, 101 (2010) 2436-2442.
[17] J. Fermoso, L. He, D. Chen, Production of high purity hydrogen by sorption enhanced steam reforming of crude glycerol, Int J Hydrogen Energy, 37 (2012) 14047-14054.
[18] N. Hajjaji, I. Baccar, M.-N. Pons, Energy and exergy analysis as tools for optimization of hydrogen production by glycerol autothermal reforming, Renewable Energy, 71 (2014) 368-380.
[19] T. Valliyappan, D. Ferdous, N.N. Bakhshi, A.K. Dalai, Production of Hydrogen and Syngas via Steam Gasification of Glycerol in a Fixed-Bed Reactor, Topics in Catalysis, 49 (2008) 59-67.
[20] M.S. Ardi, M.K. Aroua, N.A. Hashim, Progress, prospect and challenges in glycerol purification process: A review, Renewable and Sustainable Energy Reviews, 42 (2015) 1164-1173.
[21] M. Ayoub, A.Z. Abdullah, Critical review on the current scenario and significance of crude glycerol resulting from biodiesel industry towards more sustainable renewable energy industry, Renewable and Sustainable Energy Reviews, 16 (2012) 2671-2686.
[22] D. Kunii, O. Levenspiel, Fluidization Engineering, second ed., Butterworth-Heinemann, Oxford, 1992.
[23] S. Adhikari, S. Fernando, S. Gwaltney, S. Filipto, R. Markbricka, P. Steele, A. Haryanto, A thermodynamic analysis of hydrogen production by steam reforming of glycerol, Int J Hydrogen Energy, 32 (2007) 2875-2880.
[24] S. Authayanun, A. Arpornwichanop, Y. Patcharavorachot, W. Wiyaratn, S. Assabumrungrat, Hydrogen production from glycerol steam reforming for low- and high-temperature PEMFCs, Int J Hydrogen Energy, 36 (2011) 267-275.
[25] Y. Li, W. Wang, B. Chen, Y. Cao, Thermodynamic analysis of hydrogen production via glycerol steam reforming with CO_2 adsorption, Int J Hydrogen Energy, 35 (2010) 7768-7777.

[26] J.M. Silva, M.A. Soria, L.M. Madeira, Challenges and strategies for optimization of glycerol steam reforming process, Renewable and Sustainable Energy Reviews, 42 (2015) 1187-1213.
[27] X.D. Wang, S.R. Li, H. Wang, B. Liu, X.B. Ma, Thermodynamic Analysis of Glycerin Steam Reforming, Energy & Fuels, 22 (2008) 4285-4291.
[28] N. Hajjaji, A. Chahbani, Z. Khila, M.-N. Pons, A comprehensive energy–exergy-based assessment and parametric study of a hydrogen production process using steam glycerol reforming, Energy, 64 (2014) 473-483.
[29] X. Hu, G. Lu, Investigation of the steam reforming of a series of model compounds derived from bio-oil for hydrogen production, Applied Catalysis B: Environmental, 88 (2009) 376-385.
[30] A. Iulianelli, P. Ribeirinha, A. Mendes, A. Basile, Methanol steam reforming for hydrogen generation via conventional and membrane reactors: A review, Renewable and Sustainable Energy Reviews, 29 (2014) 355-368.
[31] H. Chen, Y. Ding, N.T. Cong, B. Dou, V. Dupont, M. Ghadiri, P.T. Williams, A comparative study on hydrogen production from steam-glycerol reforming: thermodynamics and experimental, Renewable Energy, 36 (2011) 779-788.
[32] B. Dou, Y. Song, C. Wang, H. Chen, Y. Xu, Hydrogen production from catalytic steam reforming of biodiesel byproduct glycerol: Issues and challenges, Renewable and Sustainable Energy Reviews, 30 (2014) 950-960.
[33] A.A. Zardini, I. Riipinen, I.K. Koponen, M. Kulmala, M. Bilde, Evaporation of ternary inorganic/organic aqueous droplets: Sodium chloride, succinic acid and water, Journal of Aerosol Science, 41 (2010) 760-770.
[34] R.P.B. Ramachandran, G. van Rossum, W.P.M. van Swaaij, S.R.A. Kersten, Evaporation of Biomass Fast Pyrolysis Oil: Evaluation of Char Formation, Environmental Progress & Sustainable Energy, 28 (2009) 410-417.
[35] C. Font Palma, A.D. Martin, Inorganic constituents formed during small-scale gasification of poultry litter: A model based study, Fuel Processing Technology, 116 (2013) 300-307.
[36] P. Nanou, H.E. Gutiérrez Murillo, W.P.M. van Swaaij, G. van Rossum, S.R.A. Kersten, Intrinsic reactivity of biomass-derived char under steam gasification conditions-potential of wood ash as catalyst, Chemical Engineering Journal, 217 (2013) 289-299.
[37] R.H. Perry, D.W. Green, Perry's Chemical Engineers' Handbook, McGraw-Hill, New York, 2008.
[38] S. Zhu, Y. Zhu, X. Gao, T. Mo, Y. Zhu, Y. Li, Production of bioadditives from glycerol esterification over zirconia supported heteropolyacids, Bioresource technology, 130 (2013) 45-51.
[39] L. Di Felice, C. Courson, P.U. Foscolo, A. Kiennemann, Iron and nickel doped alkaline-earth catalysts for biomass gasification with simultaneous tar reformation and CO_2 capture, Int J Hydrogen Energy, 36 (2011) 5296-5310.
[40] R. Trane, S. Dahl, M.S. Skjøth-Rasmussen, A.D. Jensen, Catalytic steam reforming of bio-oil, Int J Hydrogen Energy, 37 (2012) 6447-6472.
[41] M. De Torres, G. Jiménez-osés, J.A. Mayoral, E. Pires, M. de los Santos, Glycerol ketals: Synthesis and profits in biodiesel blends, Fuel, 94 (2012) 614-616.

FIGURE CAPTIONS

Fig. 1 Evolution with temperature of the thermodynamic concentration (vol.%) of H_2 (a), CO_2 (b), CO (c) and CH_4 (d) for the reforming of a 30 wt.% glycerol aqueous solution without impurities and two 30 wt.% glycerol aqueous solutions, one having 3 wt.% of CH_3COOH and the other 5 wt.% of CH_3OH.

Fig. 2 Carbon Conversion to gas (a), liquid (b) and solid (c) obtained during the reforming experiments. Results are presented as the overall values obtained in each one of the 3 h of experiment and expressed as mean ± 0.5 Fisher LSD intervals with 95% confidence.

Fig. 3 Interaction plots between CH_3OH and KOH for the initial CC gas (a and b) and CC solid (c and d) without and with CH_3COOH, respectively. Bars are LSD intervals with 95% confidence.

Fig. 4 Relative amount (vol.%) of H_2 (a), CO_2 (b) CO (c) and CH_4 (d) in the gas obtained during the reforming experiments. Results are presented as the overall values obtained in each one of the 3 h of experiment and expressed as mean ± 0.5 Fisher LSD intervals with 95% confidence.

Fig. 5 Relative amount (% chromatographic area) of aldehydes (a), alcohols (b), ketones (c), phenols (d), and cyclic compounds (e) obtained during the reforming experiments. Results are presented as the overall values obtained in each one of the 3 h of experiment and expressed as mean ± 0.5 Fisher LSD intervals with 95% confidence.

TABLES

Table 1. Response variables. Definitions and analytical techniques used in their determination.

Product	Response variable	Analytical method
Gas	$CC\ gas\ (\%) = \frac{C\ in\ the\ gas\ (g)}{C\ fed\ (g)}\ 100$	Micro Gas Chromatograph (Micro GC). N_2 as internal standard
	$Composition\ (vol.\%) = \frac{mol\ of\ each\ gas}{total\ mol\ of\ gas}\ 100$	Online analyses
Liquid	$CC\ liq\ (\%) = \frac{C\ in\ the\ liquid\ products\ (g)}{C\ fed\ (g)}\ 100$	Total Organic Carbon (TOC).
	$Composition\ (area\ \%) = \frac{area\ of\ each\ compound}{total\ area}\ 100$	GC-MS (Gas Chromatography-Mass Spectroscopy).
	$X\ gly\ (\%) = \frac{glycerol\ fed\ (g) - glycerol\ in\ the\ liquid\ (g)}{glycerol\ fed\ (g)}\ 100$	GC-FID (Gas Chromatography-Flame ionization detector)
		Offline analyses
Solid	$CC\ sol\ (\%) = 100 - CC\ gas\ (\%) - CC\ liq^{*}\ (\%)$	Elemental Analysis.
	$CC\ coke\ (\%) = \frac{C\ on\ the\ catalyst\ (g)}{C\ fed\ (g)}\ 100$	Offline analysis
	$CC\ char\ (\%) = CC\ sol\ (\%) - CC\ coke\ (\%)$	
	$\mathrm{C\ (mg\ /g\ cat.\ g\ org.)} = \frac{C\ on\ the\ catalyst\ (g) * 1000}{\mathrm{g\ catalyst\ g\ organics\ reacted}}$	

CC liq = Carbon conversion to liquid products (unreacted glycerol free).

CC liq* = Carbon conversion to liquids including unreacted glycerol

Table 2. Thermodynamic gas composition results for the simulations. The gas composition is expressed as the 95% confidence interval for the mean.

Simulation	HAc (wt.%)		MeOH (wt.%)		T (ºC)		S/C (mol H_2O/mol C)	H_2 (vol.%)	CO_2 (vol.%)	CO (vol.%)	CH_4 (vol.%)
	Codec	Actual	Codec	Actual	Codec	Actual					
1, 2, 3	-1	0	-1	0	-1	400	3.98	51.31 – 51.34	32.55– 32.56	0.72 – 0.73	10.36 – 10.39
4, 5, 6	1	3	-1	0	-1	400	3.45	48.74 – 48.77	33.34 – 33.35	0.77 – 0.78	17.09 – 17.12
7, 8, 9	-1	0	1	5	-1	400	3.18	48.29 – 48.32	31.83 – 31.84	0.77 – 0.78	19.05 – 19.08
10, 11, 12	1	3	1	5	-1	400	2.79	45.86 – 45.89	32.61 – 32.62	0.82 – 0.83	20.65 – 20.68
13, 14, 15	-1	0	-1	0	1	700	3.98	67.23 – 67.26	23.61 – 23.62	9.11 – 9.12	0.00 – 0.028
16, 17, 18	1	3	-1	0	1	700	3.45	66.58 – 66.61	23.14 – 23.15	10.23 – 10.24	0.00 – 0.028
19, 20, 21	-1	0	1	5	1	700	3.18	67.58 – 67.61	21.48 – 21.49	10.88 – 10.89	0.007 – 0.038
22, 23, 24	1	3	1	5	1	700	2.79	66.90 – 66.93	20.99 – 21.00	12.04 – 12.05	0.017 – 0.048
25, 26, 27	0	1,5	0	2,5	0	550	3.31	67.06 – 67.07	26.07 – 26.08	5.52 – 5.53	1.31 – 1.33
28, 29, 30	-1	0	0	2,5	0	550	3.55	67.59 – 67.61	26.08 – 26.09	5.21 – 5.22	1.08 – 1.11
31, 32, 33	1	3	0	2,5	0	550	3.10	66.58 – 66.60	26.04 – 26.05	5.84 – 5.85	1.49 – 1.52
34, 35, 36	0	1,5	-1	0	0	550	3.70	67.22 – 67.24	26.81 – 26.82	5.03 – 5.04	0.90 – 0.93
37, 38, 39	0	1,5	1	5	0	550	2.98	66.82 – 66.84	25.39 – 25.40	6.01 – 6.02	1.73 – 1.76
40, 41, 42	0	1,5	0	2,5	-1	400	3.31	48.54 – 48.57	32.57 – 32.58	0.77 – 0.78	18.07 – 18.10
43, 44, 45	0	1,5	0	2,5	1	700	3.31	67.12 – 67.14	22.28 – 22.29	10.55 – 10.56	0.00 – 0.023

Table 3. Relative influence of the studied variables and interactions on the thermodynamic composition of the gas according to the ANOVA analysis

	R^2	Inter.	[Ac]	[Me]	T	[Ac]*[Me]	[Ac]*T	[Me]*T	$[Ac]^2$	$[Me]^2$	T^2	[Ac]*[Me]*T	$[Ac]^2$*T	[Ac]*T^2	[Me]*T^2
H_2 (vol%)	1	67.08	-0.51 (4)	-0.20 (3)	9.29 (52)	0.014 (0.07)	0.46 (2)	0.82 (4)	0.017 (0.04)	-0.048 (0.11)	-9.24 (32)	-0.021 (0.11)	-0.027 (0.06)	-0.29 (1)	-0.45 (1)
CO_2 (vol.%)	1	26.07	-0.02 (1)	-0.71 (10)	-5.14 (69)	0 (0.05)	-0.32 (4)	-0.35 (4)	0 (0.06)	0.034 (0.21)	1.36 (11)	-0.001 (0.02)	0.006 (0.04)	0.1 (1)	-0.006 (0.03)
CO (vol.%)	1	5.53	0.31 (5)	0.49 (7)	4.48 (76)	0.005 (0.07)	0.27 (4)	0.44 (6)	0.005 (0.05)	0 (0)	0.14 (1)	0.005 (0.07)	0.007 (0.02)	-0.017 (0.11)	-0.03 (0.05)
CH_4 (vol.%)	1	1.31	0.20 (2)	0.42 (5)	-9.04 (55)	-0.015 (0.08)	-0.42 (2)	-0.90 (5)	-0.01 (0.06)	0.02 (0.02)	7.73 (29)	0.018 (0.1)	0.020 (0.02)	0.21 (1)	0.49 (1)

[Ac], [Me], T. Acetic acid concentration, methanol concentration and temperature in codec factors (-1 to +1)

Numbers in brackets indicate the percentage Pareto influence of each factor on the response variable. Pareto values represent the percentage of the orthogonal estimated total value

Response in terms of codec factors = Inter.+ [Ac] * (Ac term) + [Me] * (Me term) + T * (T term) + [Ac] * [Me] (Ac*Me term) + [Ac] * T * (Ac * T term) + [Me] * T *(Me * T term) + $[Ac]^2$ * (Ac^2 term) + $[Me]^2$ * (Me^2 term) + T^2 * (T^2 term) + [Ac] * [Me] * T * (Ac * Me * T term) + $[Ac]^2$ * T * (Ac^2 * T term) + [Ac] * T^2 * (Ac * T^2 term) + + [Me] * T^2 *(Me * T^2 term)

Table 4. Concentration (wt.%) of acetic acid, methanol potassium hydroxide (expressed in codec and actual values), pH (mean ± standard deviation) and S/C ratio of the 30 wt.% glycerol solutions

Run	$[CH_3COOH]$ (wt.%)		$[CH_3OH]$ (wt.%)		[KOH] (wt.%)		pH	S/C (mol H_2O/mol C)
	Codec	Actual	Codec	Actual	Codec	Actual		
1	-1	0	-1	0	-1	0	5.76 ± 0.22	3.98
2	1	3	-1	0	-1	0	2.46 ± 0.06	3.45
3	-1	0	1	5	-1	0	6.46 ± 0.30	3.18
4	1	3	1	5	-1	0	2.53 ± 0.22	2.79
5	-1	0	-1	0	1	2.8	13.29 ± 0.41	3.82
6	1	3	-1	0	1	2.8	11.84 ± 0.31	3.31
7	-1	0	1	5	1	2.8	13.40 ± 0.47	3.05
8	1	3	1	5	1	2.8	11.93 ± 0.37	2.66
9,10,11	0	1.5	0	2.5	0	1.4	6.50 ± 0.06	3.24

Table 5. Relative influence of the impurities on the CC gas, CC sol and CC liq during the first hour of experiment according to the ANOVA analysis

Response	R^2	Independent term	[AcH]	[MeOH]	[KOH]	[AcH] * [MeOH]	[AcH] * [KOH]	[MeOH] *[KOH]	[AcH] * [MeOH] * [KOH]
CC gas (%)	**0.97**	88.71	-2.39 (15)	4.61 (28)	-4.58 (28)	n.s.	n.s.	2.19 (13)	-2.48 (15)
CC sol. (%)	**0.95**	10.53	2.46 (15)	-4.47 (27)	4.65 (28)	n.s.	n.s.	-2.24 (14)	2.50 (15)
CC liq. (%)	n.a	1.50	n.s.	n.s.	n.s.	n.s.	n.s.	n.s.	n.s.

n.s. Not significant with 95% confidence

n.a. Not analysed

Response in terms of codec factors = Independent term + AcH term * [AcH] + MeOH term * [MeOH] + KOH term * [KOH] + AcH*MeOH term * [AcH]*[MeOH] + AcH*KOH term * [AcH]*[KOH] + AcH*MeOH*KOH term *[AcH]* [MeOH]*[KOH]

Numbers in brackets indicate the percentage Pareto influence of each factor on the response variable. Pareto values represent the percentage of the orthogonal estimated total value

Table 6. Solid carbon distribution. Overall carbon conversion to solid, char and coke and C deposited on the catalyst during three hours of experiment.

Run	1	2	3	4	5	6	7	8	9,10,11
CC solid (%)	3.93^{B}	14.22^{AB}	1.44^{B}	4.46^{B}	9.48^{AB}	19.16^{A}	6.02^{B}	7.80^{AB}	6.86 ± 2.14^{B}
CC char (%)	3.19^{B}	13.39^{AB}	0.63^{B}	4.23^{B}	9.25^{AB}	18.85^{A}	5.62^{B}	7.56^{AB}	6.54 ± 2.14^{B}
CC coke (%)	0.73^{AB}	0.82^{A}	0.81^{A}	0.22^{C}	0.22^{C}	0.31^{C}	0.41^{BC}	0.24^{C}	0.32 ± 0.07^{C}
mg C/g cat. g org.	0.90^{AB}	1.13^{A}	0.96^{AB}	0.27^{C}	0.83^{B}	0.44^{C}	0.50^{C}	0.31^{C}	0.45 ± 0.04^{C}

A,B and C in each column represents statistically significant groups with 95% confidence.

Table 7. Relative influence of the impurities on the gas composition obtained during the first hour of experiment according to the ANOVA analysis

Response	R^2	Independent term	[AcH]	[MeOH]	[KOH]	[AcH]* [MeOH]	[AcH]* [KOH]	[MeOH] *[KOH]	[AcH] * [MeOH]*[KOH]
H_2 (vol.%)	0.98	68.31	-0.56	-0.39	0.30	0.49	0.21	0.23	0.16
			(24)	(17)	(13)	(21)	(9)	(10)	(7)
CO_2 (vol.%)	0.86	25.90	0.27	-0,52	ns	-0.30	-0.33	-0.40	ns
			(15)	(28)		(16)	(18)	(22)	
CO (vol.%)	0.78	4.57	ns	0.41	ns	ns	ns	ns	-0.25
			na	na	na	na	na	na	na
CH_4 (vol.%)	0.97	1.22	0.18	0.49	ns	-0.13	ns	ns	ns
			(22)	(61)		(16)			

[ns] Not significant with 95% confidence

[na] Not analysed

Response in terms of codec factors = Independent term + AcH term * [AcH] + MeOH term * [MeOH] + KOH term * [KOH] + AcH*MeOH term * [AcH]*[MeOH] + AcH*KOH term * [AcH]*[KOH] + AcH*MeOH*KOH term *[AcH]* [MeOH]*[KOH]

Numbers in brackets indicate the percentage Pareto influence of each factor on the response variable. Pareto values represent the percentage of the orthogonal estimated total value

FIGURES

Fig. 1

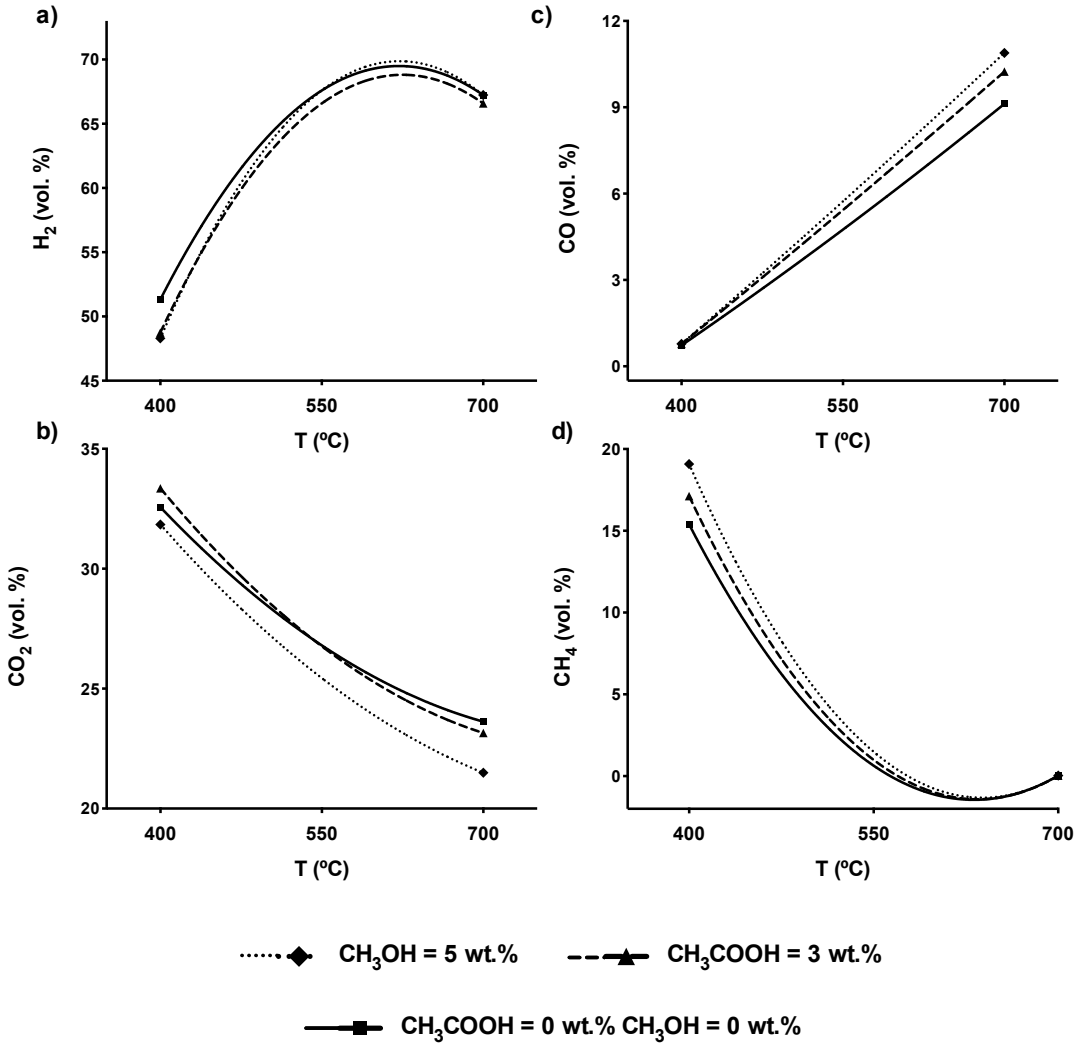

Fig. 2

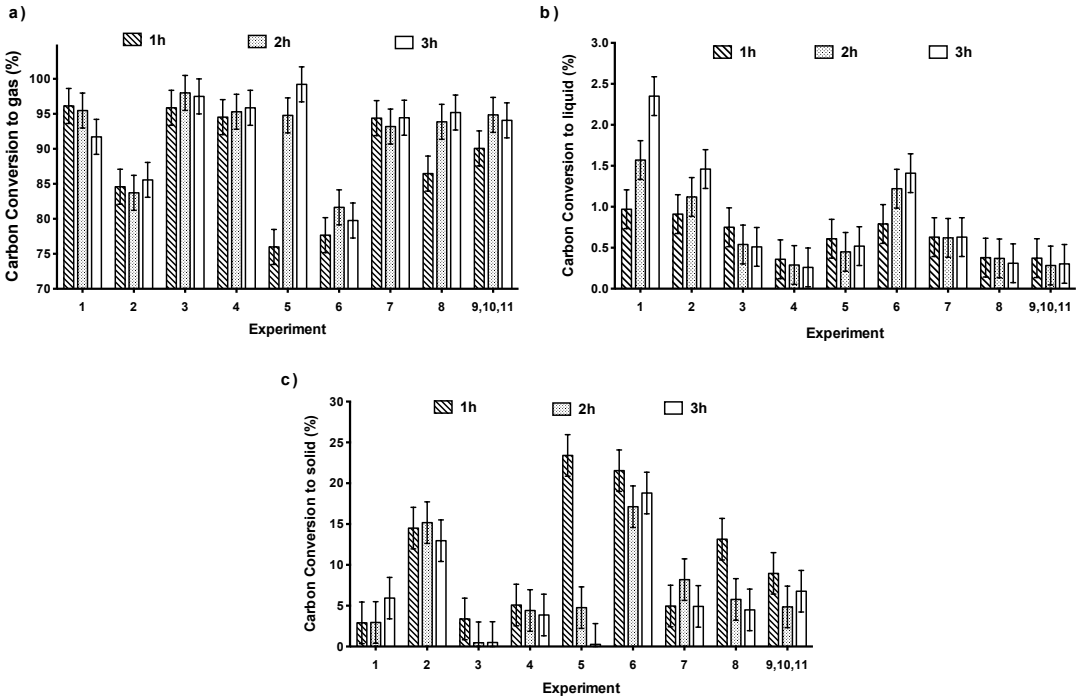
a)
1h
2h
3h
Carbon Conversion to gas (%)
100
95
90
85
80
75
70
1
2
3
4
5
6
7
8
9,10,11
Experiment
b)
1h
2h
3h
Carbon Conversion to liquid (%)
3.0
2.5
2.0
1.5
1.0
0.5
0.0
1
2
3
4
5
6
7
8
9,10,11
Experiment
c)
1h
2h
3h
Carbon Conversion to solid (%)
30
25
20
15
10
5
0
1
2
3
4
5
6
7
8
9,10,11
Experiment

Fig. 3

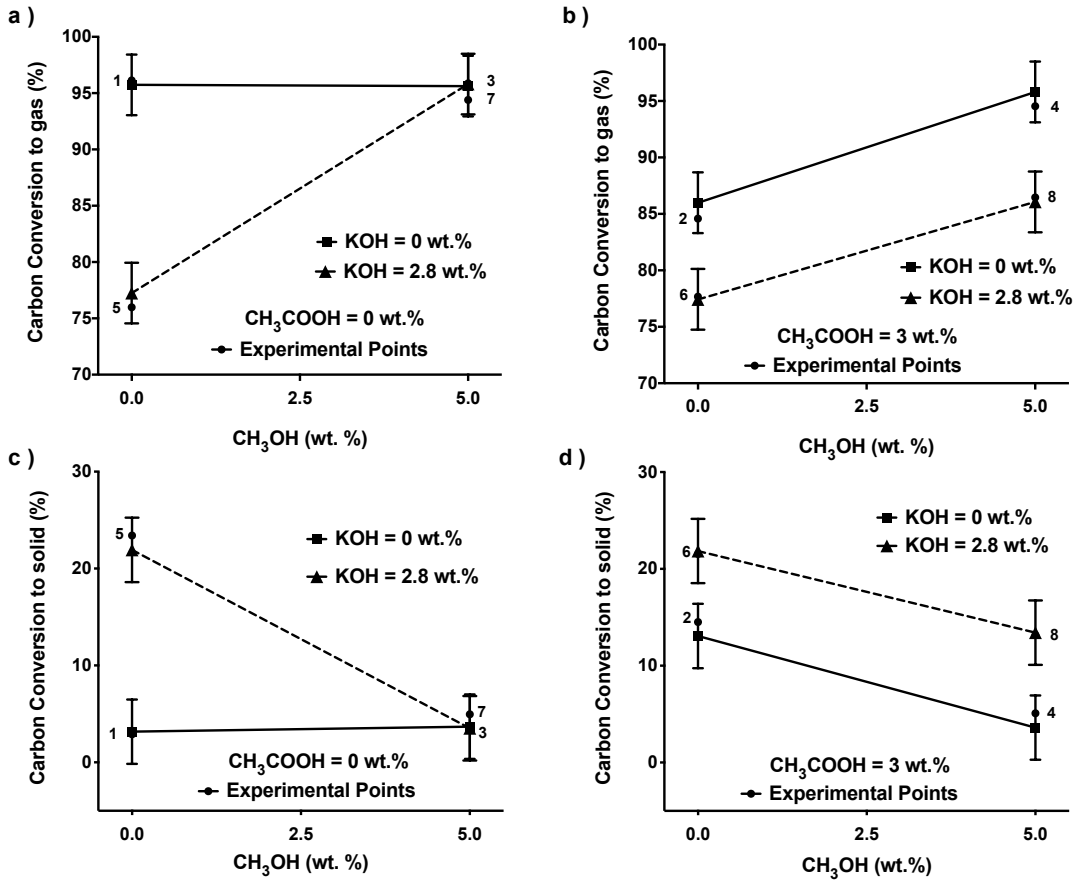
a)
Carbon Conversion to gas (%)
100
95
90
85
80
75
70
1
3
7
5
KOH = 0 wt.%
KOH = 2.8 wt.%
CH3COOH = 0 wt.%
Experimental Points
0.0
2.5
5.0
CH3OH (wt. %)
b)
Carbon Conversion to gas (%)
100
95
90
85
80
75
70
4
2
8
6
KOH = 0 wt.%
KOH = 2.8 wt.%
CH3COOH = 3 wt.%
Experimental Points
0.0
2.5
5.0
CH3OH (wt. %)
c)
Carbon Conversion to solid (%)
30
20
10
0
5
7
1
3
KOH = 0 wt.%
KOH = 2.8 wt.%
CH3COOH = 0 wt.%
Experimental Points
0.0
2.5
5.0
CH3OH (wt. %)
d)
Carbon Conversion to solid (%)
30
20
10
0
6
8
2
4
KOH = 0 wt.%
KOH = 2.8 wt.%
CH3COOH = 3 wt.%
Experimental Points
0.0
2.5
5.0
CH3OH (wt.%)

Fig.4

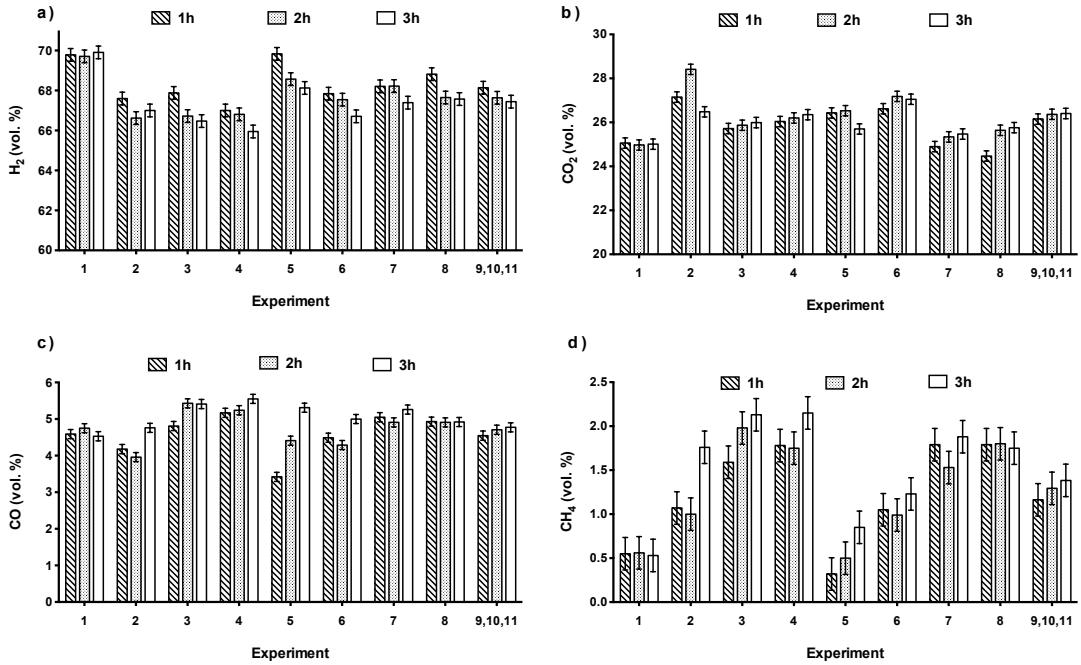
a)
1h
2h
3h
H_2 (vol. %)
Experiment
b)
CO_2 (vol. %)
c)
CO (vol. %)
d)
CH_4 (vol. %)
1
2
3
4
5
6
7
8
9,10,11

Fig. 5

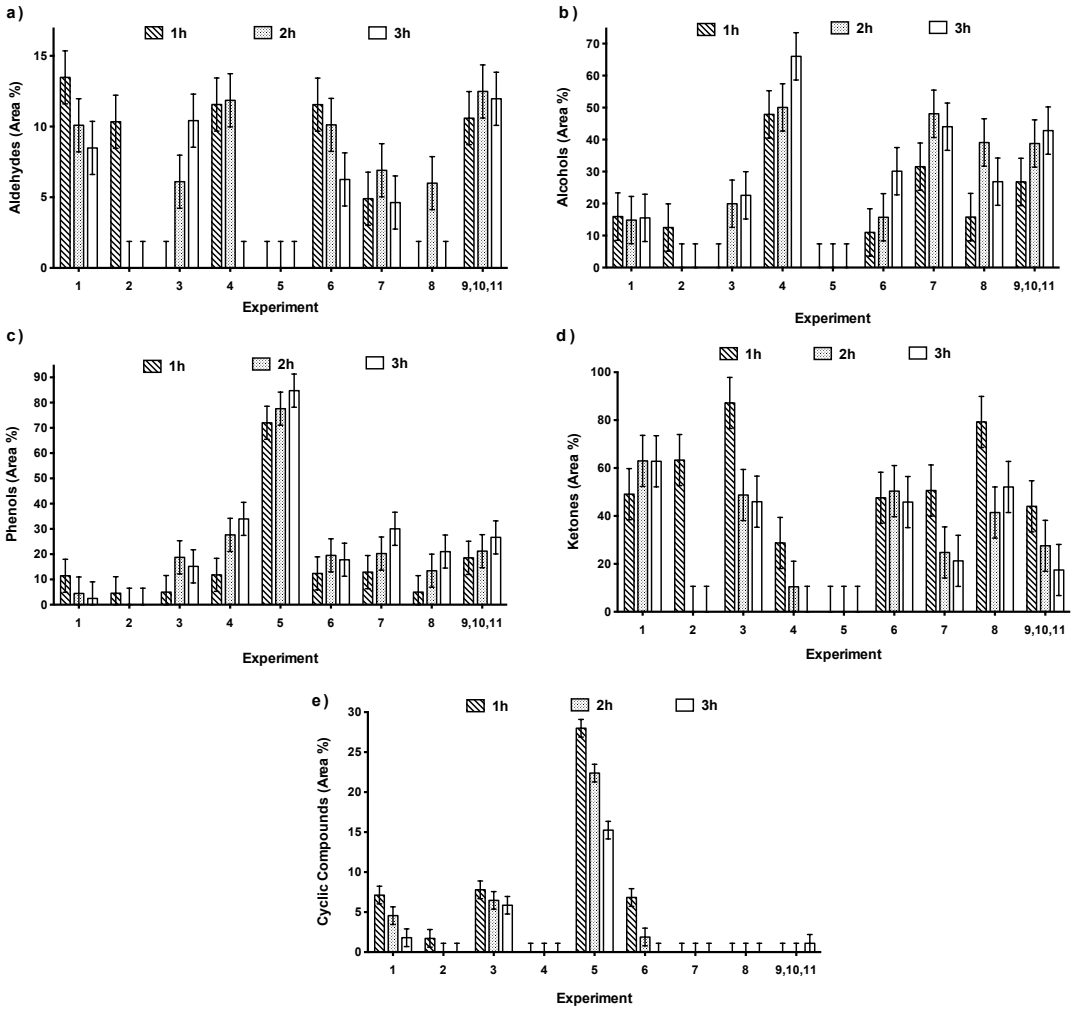
a)
1h
2h
3h
Aldehydes (Area %)
Experiment
b)
Alcohols (Area %)
c)
Phenols (Area %)
d)
Ketones (Area %)
e)
Cyclic Compounds (Area %)
1
2
3
4
5
6
7
8
9,10,11